PHYSICAL REVIEW B VOLUME 16, NUMBER 8 15 OCTOBER 1977

Absence of Anderson's transition in random lattices with off-diagonal disorder*

P. D. Antoniou
The James Franck Institute and Department of Physics, The University of Chicago, Chicago, Illinois 60637

E. N. Economou†
Department of Physics, University of Virginia, Charlottesville, Virginia 22901

(Received 9 August 1976)

Randomness is introduced in the off-diagonal elements of a tight-binding Hamiltonian. The question of localization is examined in this model Hamiltonian using two different methods: The localization function method and a self-consistent method based on an integral equation for the probability distribution of the self-energy. It is found, using both methods, that the presence of only off-diagonal randomness leaves the states in a finite region around the middle of the band always extended. Possible applications of this result are discussed.

I. INTRODUCTION

Transport properties of disordered materials are closely related to the localization character of the eigenstates of the system under consideration. A considerable effort has therefore been made to determine this character in a number of systems represented by model Hamiltonians that are simple enough to allow quantitative calculations but at the same time are believed to contain the essential physics. The localization problem has been studied almost exclusively via Anderson's model[1] of a disordered lattice. This model Hamiltonian is a tight-binding one,

$$H=\sum_n |n\rangle\epsilon_n\langle n| + \sum_{nm}{}' |n\rangle V_{nm}\langle m|, \tag{1.1}$$

the sites $\{n\}$ forming a periodic lattice. Disorder is usually introduced by assuming that $\{\epsilon_n\}$ are random variables and that $V_{nm}=V$ for nearest neighbors, zero otherwise. The role of the above, so-called "diagonal," disorder on the localization of the eigenstates of H has been studied extensively. In one dimension in particular, all states are localized no matter how small the diagonal disorder is.[2] Randomness in the off-diagonal matrix elements $\{V_{nm}\}$, "off-diagonal" randomness, has not been studied in connection with the localization problem up to now. There has been no explicit justification for this, but it has been supposed that off-diagonal and diagonal randomness would have similar effects on the localization character of the eigenstates. Recent work[3] shows that purely off-diagonal disorder leaves the eigenstate in the middle of the band (and only this one) extended in one dimension in contrast to diagonal disorder.

It therefore became apparent that such an assumption of qualitatively similar effects of diagonal and off-diagonal disorder on the localization of the eigenstates cannot be made any longer. It also became necessary to investigate the possibility of more profound differences between the two, for two-dimensional and three-dimensional lattices. In this paper we examine the role of off-diagonal disorder on the localization of the states within the framework of an Anderson Hamiltonian. In Sec. II, we discuss the modification of the localization-function method[4] necessary to include off-diagonal disorder. Section III deals with an alternative way to examine the same problem, a self-consistent method,[5] again modified to incorporate off-diagonal disorder. Section IV contains the numerical calculations and results using the analysis of the previous two sections. Both methods give the same qualitative results. The main feature is that the states around the middle of the band always remain extended in the presence of purely off-diagonal randomness. Discussion of possible applications of our results and conclusions are finally presented in Sec. V.

II. $L(E)$ METHOD

We consider a particle in the state $|\vec{0}\rangle$ at $t=0$, and following the analysis developed in the localization function method,[4,6] we examine the probability $P_{\vec{0}\vec{0}}$ of finding the particle in the state $|\vec{0}\rangle$ at $t=\infty$. $P_{\vec{0}\vec{0}}\neq 0$ implies localized states while $P_{\vec{0}\vec{0}}=0$ means that the states are extended.

It can be shown that

$$P_{\vec{0}\vec{0}}=\lim_{s\to 0^+}\frac{s}{\pi}\int_{-\infty}^{+\infty}\frac{\mathrm{Im}G_{\vec{0}}(E-is)}{2is-[\Delta_{\vec{0}}(E+is)-\Delta_{\vec{0}}(E-is)]}, \tag{2.1}$$

where $G_{\vec{0}}$ is the diagonal matrix element of the Green's function in the $\{|\vec{n}\rangle\}$ basis and $\Delta_{\vec{0}}(z)$ the self-energy at the site $\vec{0}$ defined by $\Delta_0(E)=E-\epsilon_0-G_0^{-1}(E)$. From (2.1) it becomes apparent that one

needs to examine the properties of the self-energy. Expressing the self-energy $\Delta_0(E)$ in a renormalized perturbation series[1,4,6] (RPS), we obtain

$$\Delta_{\vec{0}}(E)=\sum_{\vec{n}\neq\vec{0}} V_{0\vec{n}}(E-\epsilon_{\vec{n}}-\Delta_{\vec{n}}^{\vec{0}})^{-1}V_{\vec{n}\vec{0}} + \sum_{\substack{\vec{n}\neq\vec{0}\\ \vec{n}'\neq\vec{n},\vec{0}}} V_{\vec{0}\vec{n}'}(E-\epsilon_{\vec{n}'}-\Delta_{\vec{n}'}^{\vec{0},\vec{n}})^{-1}V_{\vec{n}'\vec{n}}(E-\epsilon_{\vec{n}}-\Delta_{\vec{n}}^{\vec{0}})^{-1}V_{\vec{n}\vec{0}} + \cdots , \tag{2.2}$$

where $\Delta_{\vec{n}}^{\vec{0}}$ is the self-energy at site $\vec{n}$ when the site $\vec{0}$ has been removed ($\epsilon_{\vec{0}}\to\infty$). We can use (2.2) to get $\Delta_{\vec{n}}^{\vec{0}}$, $\Delta_{\vec{n}}^{\vec{0},\vec{n}}$, etc., and reinsert back to (2.2). We then get a continued-fraction-like expression[4] (the renormalized perturbation expression)

$$\Delta_{\vec{0}}(E) =\sum_{\vec{n}\neq\vec{0}} V_{\vec{0}\vec{n}}\left(E-\epsilon_{\vec{n}}-\sum V_{\vec{n}\vec{l}}\frac{1}{E-\epsilon_{\vec{l}}-\cdots}V_{\vec{l}\vec{n}}+\cdots\right)^{-1}V_{\vec{n}\vec{0}} +\cdots . \tag{2.3}$$

The method discussed in this section assumes that convergence of the RPS is equivalent to the convergence of the renormalized perturbation expression, and focuses on the convergence of the RPS. We therefore examine the probability distribution of

$$\Delta_{\vec{0}}^{(M)}(E)=\sum\prod_{i=1}^{M}\left(\frac{V_{i-1,i}}{e_i}\right)V_{M0}, \tag{2.4}$$

where $e_i=E-\epsilon_i-\Delta_{\vec{i}}^{\vec{0},\vec{1},\ldots,\vec{i}-1}$ and the sum extends over all possible terms of Mth order. Each term in Eq. (2.4) may be represented, in a diagrammatic way, by a self-avoiding polygon.[1,4,6] For a specific term j the contribution to $\Delta_{\vec{0}}^{(M)}(E)$ is

$$T_j^{(M)}=\prod_{i=1}^{M}\frac{V_{i-1,i}}{e_i}. \tag{2.5}$$

If we define $X_j^{(M)}$ as $X_j^{(M)}=\ln|T_j^{(M)}|$, it follows that

$$X_j^{(M)}=\sum_{i=1}^{M}(\ln|V_{i-1,i}|-\ln|e_i|) \tag{2.5'}$$

$$\langle X_j^{(M)}\rangle = M\ln(\tilde{V}/\tilde{e}),$$

where $\tilde{V}$ and $\tilde{e}$ are defined by

$$N\ln\tilde{V}=\sum_{i=1}^{N}\langle\ln|V_{i-1,i}|\rangle , \tag{2.6a}$$

$$N\ln\tilde{e}=\sum_{i=1}^{N}\langle\ln|e_i|\rangle . \tag{2.6b}$$

Under the assumption of strong correlation[4,6] among the $T_j^{(M)}$'s it can be shown that a non-negative function $L(E)$ can be defined, such that the Mth-order term $|\Delta_{\vec{0}}^{(M)}(E)|$ is sharply distributed around $L^M(E)$, i.e.,

$$P[L^{M-Mq}(E)<|\Delta_{\vec{0}}^{(M)}(E)|<L^{M+Mq}(E)]\xrightarrow[M\to\infty]{}1, \tag{2.7}$$

with $\frac{1}{2}<q<1$ and

$$L(E)=\lim_{M\to\infty}\left(\tilde{V}^{M+1}\sum{}'\tilde{G}_{\vec{n}_1}^{\vec{0}}\tilde{G}_{\vec{n}_2}^{\vec{0}\vec{n}_1},\cdots,\tilde{G}_{\vec{n}_M}^{\vec{0}\vec{n}_1,\ldots,\vec{n}_{M-1}}\right)^{1/M}. \tag{2.8}$$

The summation of (2.8) is over all indices $n_1,\ldots,n_M$ restricted to all self-avoiding paths of order M, starting from and ending at the site $\vec{0}$:

$$\ln\tilde{G}_{\vec{n}_i}^{\vec{0},\vec{n}_1,\ldots,\vec{n}_{i-1}}=\langle\ln|G_{\vec{n}_i}^{\vec{0},\vec{n}_1,\ldots,\vec{n}_{i-1}}|\rangle_{\rm av} =\langle\ln|(E-\epsilon_{\vec{n}_i}-\Delta_{\vec{n}_i}^{\vec{0},\ldots,\vec{n}_{i-1}})^{-1}|\rangle_{\rm av}. \tag{2.9}$$

Thus if $L(E)<1$ the RPS converges and the eigenstates are localized. If $L(E)>1$ the RPS diverges resulting to extended states. $L(E_c)=1$ defines the mobility edges.

The expression (2.8) for $L(E)$ is too complicated for quantitative calculation. First, it contains an infinite number of Green's functions, and second, in general, all the $G_{\vec{n}_i}^{0,n_1,\ldots,n_{i-1}}$ cannot be calculated. Thus Licciardello and Economou[4] introduced the additional approximation (which is very good as can be seen by explicit numerical checks[4]) $G_{\vec{n}_i}^{\vec{0},\vec{n}_1,\ldots,\vec{n}_{i-1}}\simeq G_{\vec{n}_i}^{\vec{n}_{i-1}}$ and finally our expression reduces to

$$L(E)=K\tilde{V}\tilde{G}_{\vec{n}_i}^{\vec{n}_{i-1}}, \tag{2.10}$$

where $\tilde{G}_{\vec{n}}^{\vec{n}_{i-1}}(E)$ is the logarithmic average of the $\vec{n}_i$-site Green's function with the $\vec{n}_{i-1}$ site excluded, K the connectivity of the lattice, and $\tilde{V}$ is given by (2.6a).

As it has been pointed out already[4] there are pathological probability distributions, for which the expression (2.8) for $L(E)$ fails. The assumption of strong correlations for the $T_j^{(M)}$'s effectively takes into account the contributions from all "typical" paths, neglecting contributions from a very small number of highly "irregular" paths (this is done in practice by ignoring the long tails in the distribution of the $T_j^{(M)}$'s). In most cases the error introduced by this approximation is very small. Nevertheless if the contribution of the average "typical" path is zero (for some specific probability distribution), one can no longer rely on this approximation. As an example we consider the case of a binary alloy of atoms A and B, with the transfer integrals $V_{AB}=V_{BB}=0$ reflecting the fact that the overwhelming majority of paths would give zero contribution to L^M. However, it is still possible for the electrons to become delocal-

ized if they find paths of A atoms alone. The percentage of such paths tends to zero as $M \to \infty$ and they were neglected in obtaining the expression (2.8). In such a case the arithmetic average may provide a useful alternative to the logarithmic one. The arithmetic average is exact in the above described case but this is not true in general.

Returning to (2.10), for a given probability distribution for the off-diagonal matrix elements of the Hamiltonian the calculation of $\tilde{V}$ is straightforward. What remains to be calculated in (2.10) is the $\tilde{G}^{\vec{n}_i i-1}_{\vec{n}_i}(E)$. This quantity cannot be calculated exactly except for the case of diagonal only disorder with Lorentzian probability distribution of the ϵ_n's.[7] Otherwise some approximation must be employed. The most successful approximation is the coherent-potential approximation (CPA) and its extensions.[8-12] Before we give a brief presentation of the CPA we note that the expression for $L(E)$ is not actually so sensitive to the details of the approximation for $\tilde{G}^{\vec{n}_i i-1}_{\vec{n}_i}(E)$ which affect only minor quantitative features. The main qualitative features are independent of the approximations used for obtaining $\tilde{G}^{\vec{n}_i i-1}_{\vec{n}_i}$ since they stem from the continuous behavior as a function of the degree of disorder $\mathfrak{D}$ between the two extremes $\mathfrak{D} \to 0$ and $\mathfrak{D} \to \infty$ (in both extremes $\tilde{G}^{\vec{n}_i i-1}_{\vec{n}_i}$ can be calculated without the use of any approximations).

In this spirit we introduce the effective Hamiltonian[8,9,12]

$$H_e = \sum_n |n\rangle \Sigma_d \langle n| + \sum_{nm}{}' |n\rangle \Sigma_{od} \langle m| , \tag{2.11}$$

where Σ_d and Σ_{od} are complex quantities (diagonal and off-diagonal parts of the self-energy) to be determined self-consistently.

The use of an effective Hamiltonian which couples just nearest neighbors is an approximation in calculating the Green's functions. It has been shown[10] that for the case of binary alloys, with the assumption $V_{AB}^2 = V_{AA}V_{BB}$, more elaborate[11] techniques produce the same G_{00} as the simple CPA [Eq. (2.11)]. Discrepancies exist when calculating matrix elements like G_{01}. It is, however, expected that such weaknesses of the CPA extension used to treat off-diagonal disorder do not effect our results qualitatively. More sophisticated techniques are expected to introduce changes in the specific numerical results only. The details of the CPA and the results of the numerical calculations are reported in Sec. IV.

The use of the CPA leads to an explicit approximation for $L(E)$:

$$L(E) = K\tilde{V} \left| g^{\vec{n}_i i-1}_{\vec{n}_i}(E - \Sigma_d(E), \Sigma_{od}(E)) \right| , \tag{2.12a}$$

$$L(E) = K\tilde{V} \left| g_{nn}(E - \Sigma_d, \Sigma_{od}) - \frac{g_{nm}(E - \Sigma_d, \Sigma_{od}) g_{mn}(E - \Sigma_d, \Sigma_{od})}{g_{nn}(E - \Sigma_d, \Sigma_{od})} \right| , \tag{2.12b}$$

where m and n are nearest neighbors. We denote by g the periodic Green's functions corresponding to the specific lattice under consideration.

For various probability distributions for the V_{nm}'s and different types of lattices, (2.12) provides the necessary criterion for deciding whether the states are extended $[L(E) > 1]$ or localized $[L(E) < 1]$ as the energy is changed across the energy band.

III. SELF-CONSISTENT CALCULATION

In this section, we describe an alternative way[5] to deal with the localization problem, which focuses on the convergence of the iteration procedure in the RPE by approximating at the same time the RPS by its first term. Our results are a generalization of Ref. 5 to include off-diagonal disorder. Using this approximation, Eq. (2.2) for the self-energy $\Delta(E)$ reduces to

$$\Delta_i^{i-1}(z) = \sum_j V_{ij} [z - \epsilon_j - \Delta_j^{i-1}(z)]^{-1} . \tag{3.1}$$

Our notation uses the symbols $\Delta_i^{i-1}, E, \Delta_i', \Delta_i''$ instead of S_i, R, E_i, Δ_i used in the work of Ref. 5.

Self-consistency requires that the probability distribution for Δ be the same in both sides of (3.1). If $z = E + i\eta$ and $\Delta_i^{i-1} = \Delta_i' - i\Delta_i''$, one can separate the real from the imaginary parts of Δ:

$$\Delta_i' = \sum_j \frac{|V_{ij}|^2 (E - \epsilon_j - \Delta_j')}{(E - \epsilon_j - \Delta_j')^2 + (\eta + \Delta_j'')^2} , \tag{3.2a}$$

$$\Delta_i'' = \sum_j \frac{|V_{ij}|^2 (\eta + \Delta_j'')}{(E - \epsilon_j - \Delta_j')^2 + (\eta + \Delta_j'')^2} . \tag{3.2b}$$

For regions of localized states Δ_i'' approaches zero as $\eta \to 0$ except at the set of points on the real E axis corresponding to the positions of the localized states. There, introducing the quantities $\theta_i = \Delta_i''/\eta$ and taking the limit $\eta \to 0$, one can write

$$\theta_i = \sum_j \frac{|V_{ij}|^2 (1 + \theta_j)}{(E - \epsilon_j - \Delta_j')^2} . \tag{3.3}$$

Anderson[1] argued that an upper limit to the width of the probability distribution for the site energies in producing localized states can be found, if the real part of the self-energy Δ_j' is

ignored in Eq. (3.3). Using this "upper limit" approximation we obtain for θ_i

$$\theta_i = \sum_j \frac{|V_{ij}|^2(1+\theta_j)}{(E-\epsilon_j)^2}. \tag{3.4}$$

The probability distribution for θ_i is then given by

$$f(\theta_i) = \int \delta\left(\theta_i - \sum_j \frac{|V_{ij}|^2(1+\theta_j)}{(E-\epsilon_j)^2}\right) \times \prod_j f(\theta_j) p(\epsilon_j) q(V_{ij})\, d\epsilon_j\, dV_{ij}\, d\theta_j, \tag{3.5}$$

where $p(\epsilon_j)$, $q(V_{ij})$ are the probability distributions for the site energies and transfer-integrals respectively. Using the integral representation for the δ function we find for the Laplace transform of $f(\theta_i)$:

$$f_L(s) = \left[\int dx \int dV\, p(E-x) q(V) f_L\left(s\frac{V^2}{x^2}\right) e^{-sV^2/x^2}\right]^K. \tag{3.6}$$

Actually Δ_j' is correlated with θ_j in such a way that[13] $\theta_j \to \text{const} \times \Delta_j'^2$ as $\Delta_j' \to \infty$. Hence the large values of θ_i are controlled by the second-order pole in Eq. (3.3), and as result,[13] $f(\theta_i) \propto \theta_i^{-3/2}$ as $\theta_i \to \infty$.

In the approximate Eq. (3.4) large values of θ_i are dominated by (i) large values of θ_j and (ii) the shifted second-order pole if the probability for its occurrence is nonzero. The asymptotic form of $f(\theta_i)$ is thus $\theta_i^{-1-\beta}$; if the pole occurs β satisfies the inequality[5] $0 < \beta \leq 1/2$, otherwise β simply obeys the condition $0 < \beta$.

Since the position of the pole was treated very inaccurately, the present approximation can be considered self-consistent and acceptable only if it predicts that the asymptotic behavior is not determined by the pole, i.e., when $\beta < \frac{1}{2}$. One can then conclude that in the framework of the present approximation those states are localized for which β satisfying the inequality $0 < \beta < \frac{1}{2}$ exists. If $f(\theta_i) \to \theta_i^{-1-\beta}$, then $f_L(s) \to 1 - as^\beta$ as $s \to 0$; substituting in Eq. (3.6) we obtain

$$f_L(s) = 1 - aKs^\beta \int dx \int dV\, p(E-x) q(V) \left|\frac{V}{x}\right|^{2\beta}. \tag{3.7}$$

Consequently, the localized eigenstates correspond to energies satisfying the relations

$$K \iint dx\, dV\, p(E-x) q(V) \left|\frac{V}{x}\right|^{2\beta} = 1, \quad 0 < \beta < \tfrac{1}{2}. \tag{3.8}$$

Equation (3.8), in the case of off-diagonal disorder only, leads to the following equations for the mobility edge E_c:

$$K \iint dx\, dV\, p(E_c - x) q(V) \left|\frac{V}{x}\right| = 1. \tag{3.9}$$

Equation (3.9) is the condition, within the "upper limit" approximation that connects the mobility edge [introduced through $p(E_c - x)$] with the off-diagonal disorder [introduced through $q(V)$].

One can go beyond the "upper limit" approximation to include the real part of the self-energy. For $\eta \to 0$ (and therefore small Δ'' since we are in a region of localized states) Eq. (3.2b) becomes

$$\Delta_i'' = \sum_j \frac{|V_{ij}|^2 \Delta_j''}{(E - \epsilon_j - \Delta_j')^2} \tag{3.10}$$

and θ_i satisfies Eq. (3.3). We see that

$$\theta_i = \sum_j A_{ij} + \sum_j B_{ij}\theta_j, \tag{3.11a}$$

$$\Delta_i'' = \sum_j B_{ij} \Delta_j''. \tag{3.11b}$$

Equation (3.11a) possesses a solution if and only if (3.11b) does not have a nontrivial solution. Keeping this relation in mind and considering the joint probability distribution $f(\Delta_i', \Delta_i'')$, we get

$$f(\Delta_i', \Delta_i'') = \int \delta\left(\Delta_i - \sum_j \frac{|V_{ij}|^2}{E - \epsilon_j - \Delta_j'}\right) \delta\left(\Delta_i'' - \sum_j \frac{|V_{ij}|^2(\eta + \Delta_j'')}{(E - \epsilon_j - \Delta_j')^2}\right) \times P(\{V_{ij}, \epsilon_j, \Delta_j', \Delta_j''\}) \prod_j dV_{ij}\, d\epsilon_j\, d\Delta_j'\, d\Delta_j'', \tag{3.12}$$

where P is the joint probability distribution for the set of quantities $V_{ij}, \epsilon_j, \Delta_j', \Delta_j''$. We have for P

$$P(\{V_{ij}, \epsilon_j, \Delta_j', \Delta_j''\}) = \prod_j q(V_{ij}) p(\epsilon_j) f(\Delta_j', \Delta_j''). \tag{3.13}$$

Combined with (3.13), Eq. (3.12) leads to the following expression for the Fourier transform $F(k_1, k_2)$ of $f(\Delta_i', \Delta_i'')$:

$$F(k_1, k_2) = \prod_j \int dV_{ij} \int d\epsilon_j \int d\Delta_j' \int d\Delta_j''\, p(\epsilon_j) q(V_{ij}) f(\Delta_i', \Delta_i'') \exp\left(-ik_1 \frac{|V_{ij}|^2}{E - \epsilon_j - \Delta_j'} - ik_2 \frac{|V_{ij}|^2(\eta + \Delta_j'')}{(E - \epsilon_j - \Delta_j')^2}\right)$$

or, by changing variables to $x = E - \epsilon_j - \Delta_j'$, $y = \eta + \Delta_j''$,

$$F(k_1,k_2)=\left[\frac{1}{(2\pi)^2}\int dx\,dy\,dk_1'\,dk_2'\,dV\,d\epsilon\,dz\,dw f(z,w)\delta(E-\epsilon-x-z)\right.$$
$$\left.\times\delta(y-\eta-w)\exp\left(-ik_1\frac{V^2}{x}-ik_2\frac{V^2y}{x^2}\eta\right)p(\epsilon)q(V)\right]^K$$
$$=\left[\frac{1}{2\pi}\int dx\,dk_1'\,dV\,q(V)\,P(k_1')F\left(k_1',k_2\frac{V^2}{x^2}\right)\exp\left(ik_1'(E-x)-ik_2\frac{V^2}{x^2}\eta-ik_1\frac{V^2}{x}\right)\right]^K. \tag{3.14}$$

$P(k_1')$ in (3.14) is the Fourier transform of $p(\epsilon_j)$.

We examine again, as in the "upper limit" case, the behavior of $F(k_1,k_2)$ for small values of $k_2=-is$. Taking the limit of $\eta\to 0$ we observe that (3.14) becomes independent of k_2. Thus the probability distribution for the real part of the self-energy $F_0(k_1)$ obeys the following equation:

$$F_0(k_1)=\left[\frac{1}{2\pi}\int dx\,dV\,dk_1'\,q(V)P(k_1')F_0(k_1')\exp\left(ik_1'(E-x)-ik_1\frac{V^2}{x}\right)\right]^K \tag{3.15}$$

For small values of $k_2=-is$ we again expand $F_0(k_1,-is)$ as $F(k_1,-is)\simeq F_0(k_1)-B(k_1)s^{1/2}$. After some algebra we find that $B(k_1)$ satisfies the linear homogeneous integral equation

$$B(k_1)=K\tfrac{1}{2}[F_0(k_1)]^{1-1/K}\int dx\,dV\,dk_1'\,q(V)P(k_1')B(k_1')\left|\frac{V}{x}\right|\exp\left(ik_1'(E-x)-ik_1\frac{V^2}{x}\right) \tag{3.16}$$

Equation (3.16) can be transformed into a more elegant form by introducing the functions $A(x)$, $Q(x)$[5]:

$$A(x)\equiv\frac{1}{2\pi}\int P(k_1)B(k_1)\exp[ik_1(E-x)]\,dk_1, \tag{3.17a}$$

$$Q(x)\equiv\frac{1}{2\pi}\int P(k_1)[F_0(k_1)]^{1-1/K}\exp[ik_1(E-x)]\,dk_1. \tag{3.17b}$$

Then

$$A(y)=K\int dx\int dV\,q(V)\left|\frac{V}{x}\right|Q\left(y+\frac{V^2}{x}\right)A(x) \tag{3.18}$$

or

$$A(y)=K\mathfrak{L}A(x), \tag{3.19}$$

where the operator $\mathfrak{L}$ is defined as

$$\mathfrak{L}=\int dV\int dx\,q(V)Q\left(y+\frac{V^2}{x}\right)\left|\frac{V}{x}\right|. \tag{3.20}$$

For a localized state of energy E and large values of $\theta=\Delta''/\eta$ the probability distribution of θ becomes[13] proportional to $\theta^{-3/2}$, which implies that the probability distribution of Δ'', $g(\Delta'')\propto\eta^{1/2}$. It is thus apparent that

$$B(K_1)\to 0$$
$$\eta\to 0$$

or that (3.19) possesses the trivial solutions only, for localized states. Denoting by $\{\lambda_n\}$, $\{\mathfrak{u}_n\}$ the set of eigenvalues and eigenfunctions of $\mathfrak{L}$, respectively, we attempt to solve (3.19) via an iteration procedure initiated with some function $A^{(0)}=\sum_n C_n\mathfrak{u}_n$ and proceeding by applying $K_1\mathfrak{L}$, where K_1 is an as yet undefined multiplier:

$$A^{(1)}=K_1\mathfrak{L}A^{(0)}=\sum_n C_nK_1\lambda_n\mathfrak{u}_n$$
$$\vdots$$
$$A^{(N)}=K_1\mathfrak{L}A^{(N-1)}=\sum_n C_n(K\lambda_n)^N\mathfrak{u}_n. \tag{3.21}$$

If $K_1^{-1}=\Lambda_M(E)=\max\{\lambda_n\}$ the term in (3.21) containing Λ_M will dominate for large values of N, thus giving

$$\tilde{A}\equiv\lim_{N\to\infty}A^{(N)}=C_M\mathfrak{u}_M;$$

$\tilde{A}$ is a solution of Eq. (3.19). Therefore, if $K<K_1(E)$, only the trivial solution is possible for (3.19) in agreement to the original assumption that the corresponding state is localized. A continuous spectrum for the eigenvalues of $\mathfrak{L}$ implies that if $K>K_1(E)$ a nonzero solution exists and the state is extended. $K=K_1(E_c)$ determines the mobility edges.

IV. RESULTS

A. $L(E)$ method

1. Calculational details

As it is mentioned earlier $L(E)=K\tilde{V}\tilde{G}_{\vec{n}_i}^{\vec{n}_{i-1}}$. We already mentioned that, using the CPA, $\tilde{G}_{\vec{n}_i}^{\vec{n}_{i-1}}$ can be expressed in terms of Σ_d and Σ_{od} [see Eq. (2.12)], where the latter defined the effective medium.

The problem of determining Σ_d and Σ_{od} approximately has been examined in the literature.[8,9,12]

Here we present a very brief outline of a method which suits our purposes. Starting from (2.11) we proceed in this two-site generalization of the CPA by considering a pair of scatterers at sites a and b. We ignore deviations of V from Σ involving all other sites. The corresponding T matrix is now a 2×2 matrix. Using the standard techniques of scattering theory we obtain for T

$$T=\begin{pmatrix} V_{aa}-\Sigma_d & V_{ab}-\Sigma_{od} \\ V_{ba}-\Sigma_{od} & V_{bb}-\Sigma_d \end{pmatrix} \times\left[1-\begin{pmatrix} \mathcal{G}_{aa} & \mathcal{G}_{ab} \\ \mathcal{G}_{ba} & \mathcal{G}_{bb} \end{pmatrix}\begin{pmatrix} V_{aa}-\Sigma_d & V_{ab}-\Sigma_{od} \\ V_{ba}-\Sigma_{od} & V_{ba}-\Sigma_d \end{pmatrix}\right]^{-1}, \quad (4.1)$$

where $\mathcal{G}_{aa}$, $\mathcal{G}_{ab}$ are the matrix elements of the effective Green's function in the site representation. The CPA condition requires

$$\langle T\rangle=0, \quad (4.2)$$

from which Σ_d and Σ_{od} are to be determined. There are two linearly-independent equations implicit in (4.2). We chose to satisfy them in the combinations[8,9]

$$\langle T^{ab}\pm T^{aa}\rangle=0. \quad (4.3)$$

It should be pointed out here that the $\mathcal{G}$'s as well as the quantities Σ_d, Σ_{od} depend on the crystal structure, the probability distribution of ϵ_i (diagonal disorder) and the probability distribution of V_{ij} (off-diagonal disorder). For real two- and three-dimensional lattices there are no closed analytic forms for the $\mathcal{G}$'s. This of course introduces numerical difficulties in the practical determination of $\mathcal{G}$, Σ_d, and Σ_{od}. To overcome this practical problem many authors used model Green's functions that do not correspond to a real lattice but reproduce most of the important qualitative and semiquantitative features of the Green's functions for the real periodic lattices. The numerical work is thereby greatly facilitated with a minor sacrifice in quantitative accuracy.

Two of the most common model $\mathcal{G}$'s are the following:

(a) The so-called Hubbard model which gives

$$\mathcal{G}^H_{00}(E-\Sigma_d,\Sigma_{od}) =2\{E-\Sigma_d-[(E-\Sigma_d)^2-Z^2\Sigma^2_{od}]^{1/2}\}/Z^2\Sigma^2_{od}, \quad (4.4a)$$

$$\mathcal{G}^H_{0i}(E-\Sigma_d,\Sigma_{od})=[(E-\Sigma_d)\mathcal{G}^H_{00}-1]/Z\Sigma_{od} \quad (4.4b)$$

(i is a nearest neighbor of the site 0). This Green's function corresponds to an elliptically shaped density of states:

$$n(E)=(2/\pi Z^2V^2)(Z^2V^2-E^2)^{1/2}, \quad (4.5)$$

where Z is the coordination number of the lattice.

(b) The Green's function corresponding to a Bethe lattice. A Bethe lattice (or Cayley tree) is a treelike structure characterized by the connectivity constant K which is one less than the number of neighbors to a given site. (Such a structure is depicted in Fig. 1 with $K=3$.)

Then

$$\mathcal{G}^{BL}_{00}(E-\Sigma_d,\Sigma_{od})=2K/\{(K-1)(E-\Sigma_d)+(K+1)\times[(E-\Sigma_d)^2-4K\Sigma^2_{od}]^{1/2}\}, \quad (4.6a)$$

$$\mathcal{G}^{BL}_{0i}(E-\Sigma_d,\Sigma_{od})=[(E-\Sigma_d)\mathcal{G}^{BL}_{00}-1]/Z\Sigma_{od}, \quad (4.6b)$$

which gives

$$\mathcal{G}^{n-1}_n(E-\Sigma_d,\Sigma_{od}) =\{(E-\Sigma_d)-[(E-\Sigma_d)^2-4K\Sigma^2_{od}]^{1/2}\}/2K\Sigma^2_{od}. \quad (4.7)$$

(The square root must be taken with positive imaginary part to secure the correct form of $\mathcal{G}$ as $E\to\infty$.) The real lattices Green's function can be approximated by $\mathcal{G}_{BL}$ with the same Z or the same K.

In this paper calculations were done using both the Hubbard model and the Bethe-lattice Green's function. This does not imply that localization is examined in the context of a Bethe lattice. One develops a first-principles theory which leads to (2.12). It is at this level where the local properties of the specific $\mathcal{G}$ enter. As the results confirm, it makes little difference which specific Green's function is used, thus indicating that our conclusions are independent of the calculational details.

For the probability distributions of the potential, we have considered the following cases:

(i) Lorentzian :

$$P(V_{ij})=(1/\pi)V_1/[(V_{ij}-V_0)^2+V_1^2] \quad (4.8a)$$

and

$$P(\epsilon_j)=(1/\pi)\Gamma/(\epsilon_j^2+\Gamma^2). \quad (4.8b)$$

The Lorentzian probability distribution has been studied extensively in the past, but for diagonal disorder only. Thus it provides an excellent opportunity to compare the effects of off-diagonal disorder with those of diagonal. In addition it is

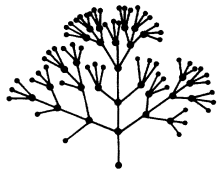

FIG. 1. Portion of a Bethe lattice with $K=3$.

easy to deal with; the CPA Eq. (4.3) determining Σ_d and Σ_{od} can be solved exactly giving

$$\Sigma_d = -i(\Gamma + V_1), \tag{4.9a}$$

$$\Sigma_{od} = V_0, \tag{4.9b}$$

independently of the lattice under consideration. For this distribution $\tilde{V}$ is easily calculated:

$$\ln\tilde{V} = \int_{-\infty}^{\infty} \ln|x|\,p(x)\,dx = \frac{V_1}{\pi}\int_{-\infty}^{\infty} \frac{\ln|x|}{(V_0-x)^2+V_1^2}\,dx$$
$$= \ln(V_0^2+V_1^2)^{1/2}, \tag{4.10}$$
$$\tilde{V} = (V_0^2+V_1^2)^{1/2}.$$

(ii) Semicircular:

$$p(V_{ij}) = (2/\pi V_1^2)[V_1^2-(V_{ij}-V_0)^2]^{1/2} \tag{4.11}$$

and no disorder for the ϵ_j's. Note that this distribution does not have the long tails of the Lorentzian. The CPA gives, for Σ_d and Σ_{od},[8]

$$\Sigma_d = \tfrac{1}{4}V_1^2 g_{00}, \tag{4.12a}$$

$$\Sigma_{od} = V_0 + \tfrac{1}{4}V_1^2 g_{0i}. \tag{4.12b}$$

The calculation for $\tilde{V}$ was performed numerically.

(iii) Binary alloy distribution: This case is physically very interesting, because it can be easily realized and rich in effects. For an alloy composed of A and B atoms of concentrations x and $1-x$, respectively, the site energies can assume two values ϵ_A and ϵ_B with probabilities x and $1-x$. The transfer integrals can take the values V_{AA}, V_{BB}, $V_{AB}=V_{BA}$ depending on what kind of atoms they connect. As it has been shown[12] if $V_{AB}^2 = V_{AA}V_{BB}$, the CPA equations take the simple form

$$x(\epsilon_A-\Sigma_d)/D_A + (1-x)(\epsilon_B-\Sigma_d)/D_B = 0, \tag{4.13a}$$

$$x(V_{AA}-\Sigma_{od})/D_A + (1-x)(V_{BB}-\Sigma_{od})/D_B = 0, \tag{4.13b}$$

where

$$D_{A(B)} = 1-(\epsilon_{A(B)}-\Sigma_d)g_{00} - (V_{AA(BB)}-\Sigma_{od})[(E-\Sigma_d)g_{00}-1]/\Sigma_{od}. \tag{4.14}$$

Before we conclude this section the following remarks should be made concerning the use of CPA and the $L(E)$ formalism:

(a) We would like to clarify first the physical interpretation of the use of the CPA. Any calculation of averages of the form $\langle G_{00}\rangle$, $\langle G_{00}G_{00}\rangle$ using CPA techniques is bound to contain errors. In a series of papers[14-16] various authors argued that predictions about the localization character of the eigenstates can be made by considering the quantity

$$P_{00}(E) = \lim_{s\to 0^+}\frac{1}{\pi s}\langle G_{00}(E+is)G_{00}(E-is)\rangle, \tag{4.15}$$

and that more generally $\langle G(E+is)G(E-is)\rangle$ determines average transport properties. The calculation of the average in (4.15) is done using CPA or some other similar technique. Such calculations conclude that localization cannot take place. This is something expected since P_{00} is a non-negative quantity, and localization is decided on whether P_{00} is zero or not. Any approximation, like the CPA, applied to a direct calculation of averages of the form (4.15), is expected to modify the outcome seriously. Small errors have a dramatic effect on the final results. On the other hand the $L(E)$ method uses the CPA at a much later stage of the calculation. It is not any more a question of comparison of a non-negative quantity with zero. It is rather the comparison of the localization function with unity. The CPA definitely has an effect on the value of the energy where $L(E_c)=1$. But it is only quantitative corrections that are now expected. The sensitivity of a direct use of CPA to calculate expressions like (4.15) is not present any more.

(b) The second point is the replacement of the logarithmic average of $|G_{n_i^{i-1}}^{n_i^i}|$ in (2.10) by its CPA analog $|g_{n_i^{i-1}}^{n_i^i}|$ in (2.12a). To first order in the T matrix the average of any function of G can be replaced by the same function of the CPA Green's function g. The truth of the above statement can be seen by considering a function of the exact G, $F(G)$. Expanding $F(G)$ we get

$$F(G) = F(g) + \left(\frac{\partial F}{\partial G}\right)_g (G-g).$$

To first order in T, $(G-g) = gTg$ which implies that

$$\langle F(G)\rangle = F(g) + \left(\frac{\partial F}{\partial G}\right)_g g\langle T\rangle g.$$

Using the CPA condition we obtain $\langle F(G)\rangle = F(g)$. To this extent, the relationship $\langle \ln|G_{n_i^{i-1}}^{n_i^i}|\rangle = \ln|g_{n_i^{i-1}}^{n_i^i}|$ which was implicitly used in deriving (2.12a) from (2.10) is justified.

2. Results

For the Lorentzian probability distribution and the Bethe-lattice model for g we obtain for $L(E)$, by combining Eqs. (2.12), (4.6), (4.8), and (4.10),

$$L(E) = \tfrac{1}{2}[1+(V_1/V_0)^2]^{1/2}\left|[E+i(\Gamma+V_1)]/V_0 - \{[E+i(\Gamma+V_1)^2/V_0]^2-4K\}^{1/2}\right|. \tag{4.16}$$

Equation (4.16) is very important because it is a simple explicit analytic expression for $L(E)$ and, though approximate, it is very successful in producing the exact behavior in several limiting cases and interpolating at least in a qualitative way successfully in between. Thus

(i) The periodic limit $V_1 = 0$, $\Gamma = 0$ is reproduced exactly ($K = Z - 1$ for a Bethe lattice).

(ii) In the special case $V_0 = 0$ the localization function becomes

$$L(E) = KV_1/[E^2 + (\Gamma + V_1)^2]^{1/2}, \tag{4.17}$$

which reproduces exactly the one-dimensional ($K = 1$) general result. For off-diagonal disorder only the $E = 0$ state may be extended. All others are predicted to be localized.[3] This is not a small achievement in view of the several approximations used and the fact that the $L(E)$ method is not really designed to treat the one-dimensional case. Note, however, that for $V_0 \neq 0$ the one-dimensional result (the $E = 0$ state is extended, all others are localized) is not reproduced. $L(E)$ has a maximum for $E = 0$ which is lower than 1 and approaches 1 only for $V_0 \to 0$ or $V_1 \to \infty$.

(iii) The $\Gamma = 0$ case (only off-diagonal randomness) is particularly interesting. The main result is that the states at and around the middle of the band, $E = 0$, are extended. This is clearly shown in Fig. 2(a). For large values of V_1, we can use (4.17) and solve for E. We find that the mobility edges become proportional to V_1:

$$E_c = \pm (K^2 - 1)^{1/2} V_1 . \tag{4.18}$$

Another interesting feature of Fig. 2(a) is that the mobility edges move inwards as the off-diagonal randomness increases from zero. Thus a neck appears in the E_c curve, i.e., as the off-diagonal disorder increases, more and more states become localized. This can be understood if we consider the probability of finding very small V_{ij}'s. We therefore examine the probability that V_{ij} belongs to the interval $[-W, W]$ with $W/V_0 \ll 1$, and we denote it by $P(-W, W)$. It can be found that

$$P(-W,W) = \int_{-W}^{W} P(V_{ij})\, dV_{ij} = \frac{1}{\pi}\left[\tan^{-1}\left(\frac{V_0 + W}{V_1}\right) - \tan^{-1}\left(\frac{V_0 - W}{V_1}\right)\right] . \tag{4.19a}$$

This probability possesses a maximum for

$$V_1/V_0 = [1 - (W/V_0)^2]^{1/2} . \tag{4.19b}$$

If we plot $P(-W, W)$ vs V_1/V_0 we get the curve (a) of Fig. 3. It is this maximum in $P(-W, W)$ that is responsible for the neck in the mobility edge curve, because as the disorder increases from

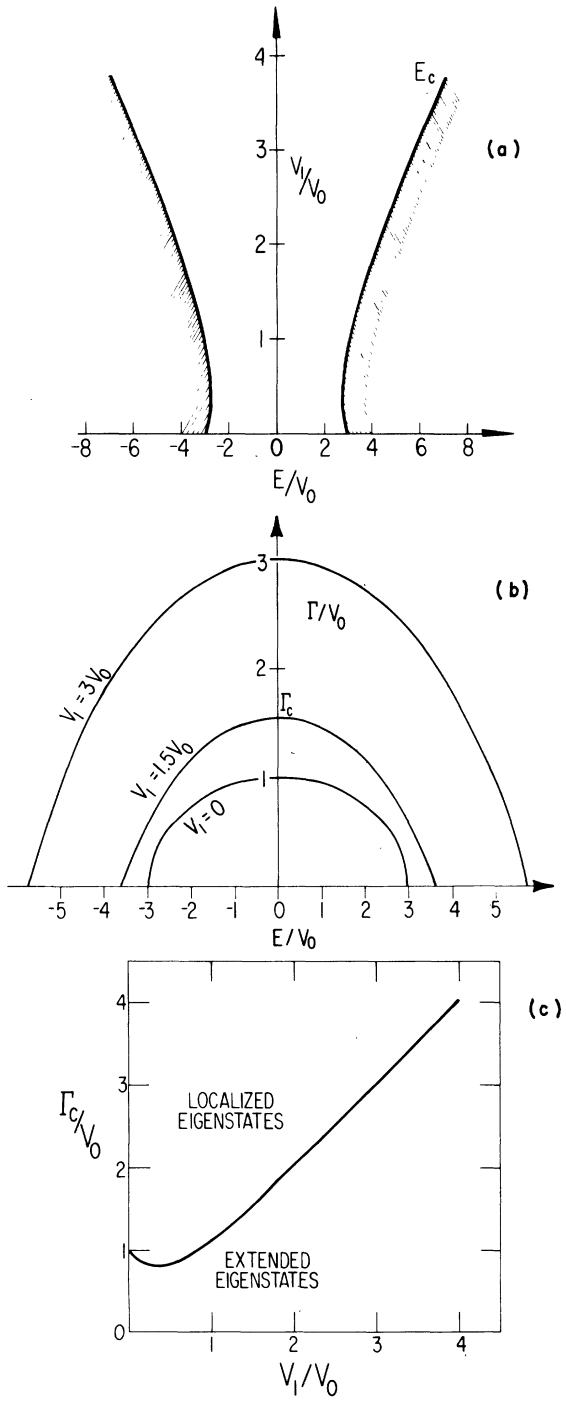

FIG. 2. (a) Mobility edge trajectories E_c as functions of off-diagonal randomness for a Lorentzian probability distribution of width V_1, centered at V_0. The Green's functions used correspond to a Bethe lattice of $K = 2$. Shaded regions contain localized states. (b) Mobility edge trajectories vs Γ, the width of the Lorentzian distribution for the diagonal disorder, and different values of V_1. The states inside the curves are extended. (c) Γ_c vs V_1, where Γ_c is the critical value of Γ for Anderson's transition.

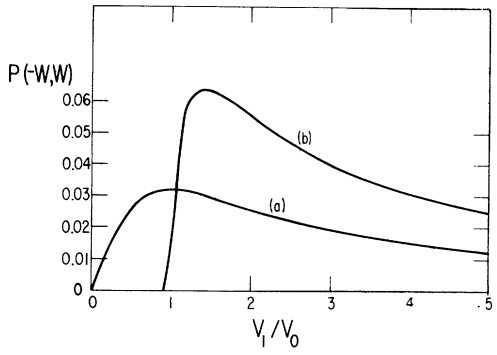

FIG. 3. Probability of finding the potential V_{ij} in the interval $[-W, W]$ for (a) a Lorentzian probability distribution; (b) a semicircular probability distribution. The value of W is $0.1V_0$.

zero it becomes more and more probable to find in the average path, V_{ij}'s small enough to stop the propagation of the electrons. As K increases, the neck becomes less pronounced and moves towards the origin, since electrons have more possibilities to escape now.

(iv) The case where $\Gamma \neq 0$ but $V_1 = 0$ (only diagonal disorder) is correctly reproduced (see Ref. 6). Such a case is presented in Fig. 2(b), where we plot the mobility edges E_c, as a function of diagonal disorder Γ, for different values of the off-diagonal randomness V_1. The $V_1 = 0$ curve corresponds to the case studied in Ref. 6. The critical value Γ_c needed to obtain the usual Anderson's transition increases with increasing V_1, according to

$$\Gamma_c/V_0 = \{K - [1 + (V_1/V_0)^2]^{-1}\} \times [1 + (V_1/V_0)^2]^{1/2} - V_1/V_0, \quad (4.20)$$

presented in Fig. 2(c). As it can be seen from (4.20) $(d\Gamma_c/dV_1)_0 = -1$ resulting in a neck for the Γ_c curve, for similar reasons as above.

Figure 4 summarizes all previous discussion. A three-dimensional space is used there with axes $(\Gamma/V_0, V_1/V_0, E/V_0)$. In this space the mobility edge is a surface $E_c/V_0 = f(V_1/V_0, \Gamma/V_0)$, defined by (4.16) and $L(E) = 1$. In the interior of this surface the eigenstates are extended while in the outside they are localized. As $V_1/V_0 \to \infty$ this surface reduces to the cone $E_c = \pm[K^2 V_1^2 - (V_1 + \Gamma)^2]^{1/2}$. As $K \to 1$ (one-dimensional case) the cone collapses to the V_1/V_0 axis, as it should.

The Lorentzian probability distribution was also combined with the Hubbard model Green's functions. The localization function was obtained by combining (2.12), (4.4), (4.9), and (4.10). The mobility edges behave as previously, with minor numerical differences for relatively small values of the parameters involved. We find as before that for large V_1 and any fixed value of Γ, the mobility

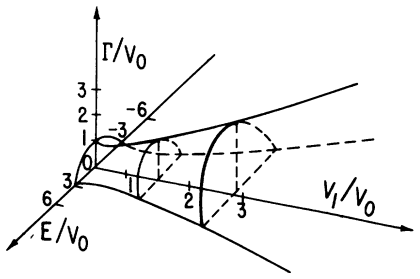

FIG. 4. Surface shows the mobility edge E_c, as a function of the width V_1, Γ of the Lorentzian probability distributions for the off-diagonal and diagonal matrix elements of the Hamiltonian. In the calculation Bethe lattice unperturbed Green's functions with $K = 2$ were used. The eigenstates inside this surface are extended, the ones outside are localized. All energies are normalized with respect to V_0, the center of the distribution for the V_{ij}'s.

edge becomes proportional to V_1: $E_c = \pm(K^2 - 1)^{1/2} V_1$.

The second probability distribution examined was the semicircular one [see Eq. (5.11)]. Using both model Green's functions [Eqs. (4.4) and (4.6)] the mobility edges were found by combining them with (2.12) and (4.12). The calculation was done numerically and gave the results presented in Fig. 5. The qualitative behavior is again the same as when a Lorentzian probability was used. The results indicate that the model Green's function used has very little effect on the mobility-edge curve, producing minor quantitative differences for the two cases (Hubbard model and Bethe-lattice model Green's function). The neck in the mobility-edge curve is now much more pronounced. It is the

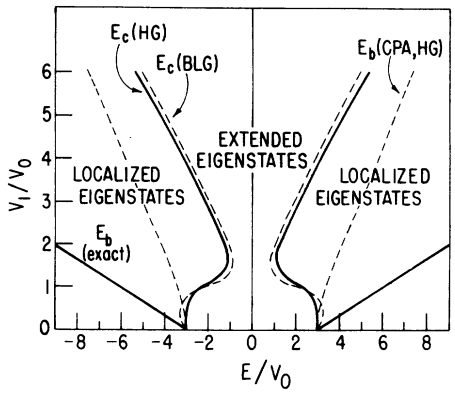

FIG. 5. Band E_b and mobility E_c edges as a function of off-diagonal randomness for a semicircular probability distribution of width V_1, centered at V_0. HG indicates the use of the Hubbard Green's function and BLG the Bethe-lattice Green's function (see text).

absence of the long tails in the semicircular distribution which is responsible for this enhancement. Now the probability maximum for finding a value for the potential V_{ij} in the interval $[-W, W]$ appears much more abruptly and is more pronounced than it was before. [Compare curve (b) of Fig. 3 with curve (a) which corresponds to the Lorentzian.] We find

$$P(-W,W)=\begin{cases}\frac{1}{\pi}\left\{\frac{\pi}{2}-\sin^{-1}\left(\frac{V_0-W}{V_1}\right)-\left(\frac{V_0-W}{V_1}\right)\left[1-\left(\frac{V_0-W}{V_1}\right)^2\right]^{1/2}\right\} & V_0-W\le V_1\le V_0+W,\\ \frac{1}{\pi}\left\{\left(\frac{V_0+W}{V_1}\right)\left[1-\left(\frac{V_0+W}{V_1}\right)^2\right]^{1/2}-\left(\frac{V_0-W}{V_1}\right)\left[1-\left(\frac{V_0-W}{V_1}\right)^2\right]^{1/2}\right. & \\ \quad\left.+\sin^{-1}\left(\frac{V_0+W}{V_1}\right)-\sin^{-1}\left(\frac{V_0-W}{V_1}\right)\right\} & V_1>V_0+W,\end{cases}$$

and the maximum appears at $V_1/V_0=2[1+(W/V_0)^2]^{1/2}$. This difference is also clearly shown in Fig. 6, where the percentage of extended states is plotted as a function of V_1/V_0. The pronounced maximum of the semicircular probability distribution produces a clear minimum in the fraction of extended states, while the much weaker maximum of the Lorentzian is not strong enough to produce such a minimum. The difference in the asymptotic values the two curves achieve for large V_1/V_0 comes from the fact that the Lorentzian possesses long tails, absent in the semicircular case. Localized states with large eigenenergies cannot exist unless the potential can also take values comparable to the energy. (Otherwise the Schrödinger equation is not satisfied.) This requirement can be satisfied always for the Lorentzian which extends to infinity, while the semicircular distribution, being a terminating one, possesses a smaller number of such localized states.

We find asymptotically, for large V_1/V_0,

$$\ln\tilde{V}=\frac{2}{\pi V_1}\int_{V_0-V_1}^{V_0+V_1}\left[1-\left(\frac{x-V_0}{V_1}\right)^2\right]^{1/2}\ln|x|\,dx$$

$$\simeq\frac{4}{\pi}\int_0^1(1-y^2)^{1/2}\ln|V_0+V_1y|\,dy,$$

and, for

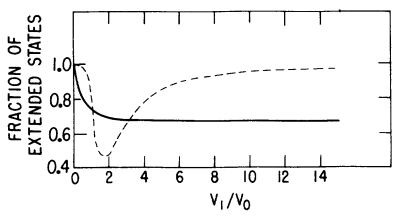

FIG. 6. Percentage of extended states vs the off-diagonal randomness V_1 for a Lorentzian probability distribution (solid line) and a semicircular probability distribution (dashed line). In both cases a Hubbard Green's function was used.

$V_1/V_0\to\infty$,

$$\ln\tilde{V}=\frac{4\ln V_1}{\pi}\int_0^1(1-y^2)^{1/2}\,dy+\frac{4}{\pi}\int_0^1(1-y^2)^{1/2}\,dy$$

or, finally,

$$\tilde{V}=V_1/2\sqrt{e}. \tag{4.21a}$$

On the other hand,

$$g_{n_i}^{n_i-1}\xrightarrow[V_1/V_0\to\infty]{}\frac{1}{E-\Sigma_d} \tag{4.21b}$$

and

$$\Sigma_d\xrightarrow[V_1/V_0\to\infty]{}\tfrac{1}{2}[E-(E^2-V_1^2)^{1/2}]\,. \tag{4.21c}$$

Using Eqs. (4.21) together with (2.12) we get for the localization function

$$L(E)\simeq(KV_1/\sqrt{e})[|E+(E^2-V_1^2)^{1/2}|]^{-1}\quad V_1/V_0\gg1. \tag{4.22}$$

Thus

$$\frac{E_c}{V_0}=\pm[(K^2+e)/2K\sqrt{e}](V_1/V_0),\quad V_1/V_0\gg1, \tag{4.23}$$

independently of the details of the lattice. As in the Lorentzian case, the mobility edge becomes proportional to the off-diagonal disorder for large values of the latter.

The $L(E)$ method was finally applied to study the character of the eigenstates of a binary alloy. Equations (4.13), together with (4.4) and (4.6) (for the two types of Green's function), were solved numerically following the most rapidly converging iteration procedure.[12] The results of the numerical calculations were fed into Eq. (2.12), and the mobility edges were determined for various concentrations x. Both the Hubbard and the Bethe-lattice model Green's function give quite similar results. In Fig. 7 we show the results for the Bethe-lattice case. The mobility edges reduce to the correct subband edges for the two limiting cases $x=0$ and $x=1$ as they should.

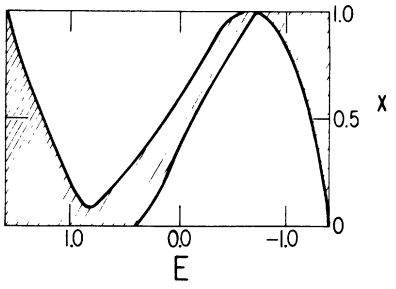

FIG. 7. Mobility edges E_c for a binary alloy as a function of the concentration x, for fixed values of diagonal and off-diagonal randomness ($\epsilon_A - \epsilon_B = 1, V_{AA} = 1.1, V_{BB} = 0.9$). Bethe-lattice unperturbed Green's functions were used. The shaded areas contain localized eigenstates.

B. Self-consistent calculation

We now present the results obtained using the analysis of Sec. III. Within the "upper limit" approximation and in the absence of diagonal disorder we get from (3.8)

$$\frac{K}{E_c}\int q(V)|V|\,dV = 1. \tag{4.24}$$

For the Lorentzian probability distribution [Eq. (4.8a)] the mobility edge is given by

$$E_c/V_0 = K[1+(V_1/V_0)^2]^{1/2}. \tag{4.25}$$

For the semicircular probability distribution [Eq. (4.11)] the mobility edge is found to be

$$\frac{E_c}{V_0} = \frac{2K}{\pi}\frac{V_1}{V_0}\int_{V_0/V_1-1}^{V_0/V_1+1}\left[1-\left(x-\frac{V_0}{V_1}\right)^2\right]^{1/2}|x|\,dx. \tag{4.26}$$

Equation (4.26) was used to calculate the mobility edges for various degrees of off-diagonal randomness V_1/V_0. The self-consistent calculation within the "upper-limit" approximation gives results qualitatively similar to those of the $L(E)$ method. Quantitative differences exist as in the case of diagonal disorder.

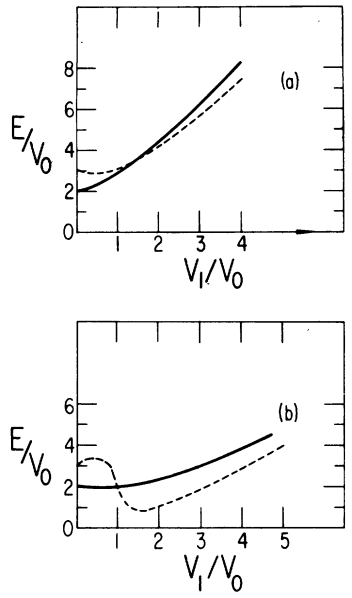

FIG. 8. Mobility-edge trajectories for off-diagonal randomness only, within the "upper limit" approximation, for a lattice of $K=2$. (a) A Lorentzian; (b) a semicircular probability distribution of width V_1, centered at V_0, is used (solid lines). The corresponding curves based on the $L(E)$ method are reproduced for comparison (dashed lines).

The main quantitative difference is that the $L(E)$ method gives more localized states than the "upper limit" approximation to the self-consistent approach. It is established[4] from numerical work on diagonal disorder that the $L(E)$ method is much more accurate than the "upper limit" method. In Fig. 8 the two methods are compared. [Solid lines represent curves obtained within the "upper limit" approximation, dashed lines are the corresponding curves for the $L(E)$ method.]

Results were also obtained using the exact Eq. (3.15) or its equivalent (3.18). In order to study (3.18) the form of $Q(y+V^2/x)$ must be found, so we study first (3.15). The x integration gives

$$\int_{-\infty}^{+\infty} e^{-ik_1'x - ik_1V^2/x}\,dx = \begin{cases} (2\pi a/k_1')J_1(-2a), & k_1k_1'>0 \text{ and } a=-(k_1k_1'V^2)^{1/2}, \\ (4\pi a/k_1')\delta(2a), & k_1k_1'<0 \text{ and } a=(-k_1k_1'V^2)^{1/2}. \end{cases}$$

J_1 is the Bessel function of the first kind. Considering again off-diagonal disorder only, the probability distribution for the ϵ_j's is a δ function and therefore its Fourier transform $P(k_1')=1$. Considering the probability distribution for the V_{ij} we examine the case $q(V)=\frac{1}{2}\lambda e^{-\lambda|V|}$ and obtain for $F_0(k_1)$, after the integrations are performed, the integral equation

$$F_0(k_1) = \left(2\lambda k_1\int_0^\infty \frac{F_0(k_1')e^{ik_1'E}dk_1'}{(\lambda^2+4k_1k_1')^{3/2}}\right)^K, \quad k_1>0, \tag{4.27a}$$

$$F_0(k_1) = \left(-2\lambda k_1\int_0^\infty \frac{F_0(-k_1')e^{-ik_1'E}}{(\lambda^2-4k_1k_1')^{3/2}}\right)^K, \quad k_1<0. \tag{4.27b}$$

For the middle of the band, $E=0$ (4.27a) becomes

$$F_0(k_1)=\left(2\lambda k_1\int_0^\infty \frac{F_0(k_1')dk_1'}{(\lambda^2+4k_1k_1')^{3/2}}\right)^K. \tag{4.28}$$

Equation (4.28) can be solved exactly with solution

$$F_0(k_1)=1. \tag{4.29}$$

Substituting (4.29) into (3.17b) we perform the integration and obtain $Q(x)=\delta(x)$. We can now use this form of $Q(x)$ into (3.18) to get

$$A(y)=K'\int A(x)\delta\left(y+\frac{V^2}{x}\right)\left|\frac{V}{x}\right|q(V)dx\,dV$$

or

$$A(y)=\tfrac{1}{2}K'\lambda|y|\int_{-\infty}^{\infty}A\left(-\frac{V^2}{y}\right)\frac{e^{-\lambda|V|}}{|V|}dV \tag{4.30}$$

or

$$A(y)=K'\lambda|y|\int_0^\infty A\left(-\frac{V^2}{y}\right)\frac{e^{-\lambda V}}{V}dV.$$

Equation (4.30) possesses the solution $A(y)=(|y|)^{1/2}$, with eigenvalue $K'=1$. We thus conclude the following: (i) The one-dimensional case is correctly reproduced. The $E=0$ state may be extended, since then $K'=K=1$. (ii) For two- or three-dimensional lattices $K>1$. Because of symmetry with respect to the center of the band ($E=0$) the eigenvalues of $\mathfrak{L}$ must be even functions of the energy. If

$$\left.\frac{d^2\Lambda_M^{-1}(E)}{dE^2}\right|_0<0,$$

$\Lambda_M^{-1}(0)$ is a maximum and all eigenstates are predicted localized for all degrees of off-diagonal randomness. We reject this possibility because it contradicts the well-known result of energy bands (extended states) in the periodic limit of large λ. If

$$\left.\frac{d^2\Lambda_M^{-1}(E)}{dE^2}\right|_0>0,$$

then $\Lambda_M^{-1}(0)$ is a minimum producing a finite region of extended eigenstates around the middle of the band for all values of λ. This result agrees with the approximate calculations and correctly contains the feature of the band in the periodic limit. This result is in agreement with the previous results, determining the localization character of the eigenstates, with the help of the $L(E)$ method. The $L(E)$ method focuses on the convergence of the RPS and examines the convergence criteria in an approximate way, ignoring the question of convergence of the continued fraction. The self-consistent method truncates the RPS and examines the continued fraction in the terms kept in detail. The two methods thus each focus on a different one of the two convergence problems arising in studying localization. As the two problems of convergence are quite distinct and as both yield qualitatively similar results for off-diagonal disorder as regards localization, we expect these results to be correct. Both methods agree on the fact that in random lattices with pure off-diagonal disorder there is no Anderson's transition.

V. CONCLUSIONS

We have investigated the localization character of the eigenstates of an Anderson type of random Hamiltonian, when off-diagonal randomness is present. It is found that diagonal and off-diagonal disorder have qualitatively different effects on the localization of the eigenstates. When only diagonal disorder is present there exists a critical value of the quantity measuring randomness such that for any randomness above this value all existing states are predicted localized. This transition to nonexistence of extended states, known as Anderson's transition, is absent in the presence of off-diagonal randomness alone. Off-diagonal disorder produces localized states at the tails of the band but not in the middle. Even though the mobility edges may initially move inwards as the disorder increases from zero, they eventually move outwards, becoming asymptotically proportional to the off-diagonal randomness for large randomness.

It should be emphasized that the two methods, namely the $L(E)$ method and the self-consistent method, built on quite different assumptions produce the same qualitative behavior for the mobility edges as a function of off-diagonal disorder. They both predict a finite region around the middle of the band, for which the states remain extended no matter how small or large the degree of disorder is. The $L(E)$ method is rather well established in dealing with the problem of diagonal disorder,[17-19] producing values in good agreement with numerical data.[20] We are therefore confident that, while the exact numbers produced in this paper might be changed, if an exact theory is developed in the future, the qualitative picture presented here will still be true, containing the basic physics of the problem. We note here that our predictions can be checked by computer experiments especially on two-dimensional lattices for which rather accurate methods have been developed.[21,22] We currently investigate this question.

The present results should have important consequences on a number of physical systems exhibiting off-diagonal disorder, such as the impurity bands in crystalline semiconductors[23] and substitutional antiferromagnets.[20,24] For the

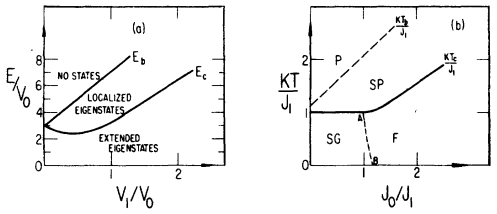

FIG. 9. (a) Band-edge (E_b) and mobility-edge (E_c) trajectories in the presence of off-diagonal disorder only, of width V_1, centered at V_0. (b) Phase diagram for the random Ising system. J_0, J_1 are the center and width respectively of the probability distribution for the J_{ij}'s. KT, J_1 and J_0 correspond to E, V_1, and V_0. P: paramagnetic phase; SP: superparamagnetic phase; F: ferromagnetic phase; SG: spin-glass phase.

former, the results of this paper show that, at least for uncompensated specimens, the electron-electron correlation and not the randomness is responsible for the observed metal-insulator transitions. Quantitative studies of this system may provide a detailed theoretical framework to analyze the host of experimental data. The system of mixed antiferromagnets, finally, can be reduced to the model of a binary alloy[20] allowing again quantitative studies and direct comparison with experiments.

The present results could be used to provide a physical understanding of certain properties of the spin-glass system. Such a system can be approximated by an Ising model with random exchange integrals J_{ij}. If we denote by σ_i the spin in the ith site and by $\langle\sigma_i\rangle$ the thermodynamic average which defines the order parameter, for low values of $\langle\sigma_i\rangle/KT$, and within the mean-field approximation, the $\langle\sigma_i\rangle$'s satisfy the matrix equation

$$KT\langle\sigma_i\rangle = \sum_j J_{ij}\langle\sigma_j\rangle . \tag{5.1}$$

Equation (5.1) is identical to the matrix equation

$$E|\psi\rangle = H|\psi\rangle . \tag{5.2}$$

The analogy is obvious if we expand $|\psi\rangle$ in terms of the local states $|i\rangle$:

$$|\psi\rangle = \sum_i a_i |i\rangle .$$

For our tight-binding Hamiltonian, we find by setting the ϵ_j's equal to zero:

$$E|i\rangle = \sum_j V_{ij}|j\rangle . \tag{5.3}$$

The analogue of E is KT and J_{ij} takes now the place of V_{ij}.

Figure 9(a) shows the electronic case as predicted by our theory. There are three distinct regions in the figure. The region where no states exist (above the band edge E_b), where (5.3) does not have a nontrivial solution, the region of localized states (between the band and mobility edge E_c), where the electron wave function is nonzero in a finite region of the lattice and the region of extended states, where the electron's wave function extends over the whole lattice. On the basis of the above equivalence between the electronic problem and the spin glass we draw Fig. 9(b). Here we follow the traditional way of presenting a phase diagram for such a system by plotting E/V_1 vs V_0/V_1, then using the analogy of E, V_0, V_1 to KT, J_0, J_1, respectively. (We remind the reader that J_0, J_1 are the center and width of the probability distribution for the J_{in}'s.) The corresponding three regions, discussed above, are denoted now by P, SP, and SG + F. In the paramagnetic (P) region there are no solutions at all, $\langle\sigma_i\rangle = 0$. The superparamagnetic (SP) region contains localized solutions, i.e., $\langle\sigma_i\rangle \neq 0$ for finite regions in the system. Such a state can be visualized as a paramagnetic matrix with magnetic particles of finite extent embedded in it. In the SG + F (spin glass and ferromagnetic) region, we predict solutions extending throughout the lattice, to be identified with the existence of long-range order.

Detailed theories[25-27] of the spin glasses produce the line separating the SP from the SG + F region with very similar shape as the one presented here. Such theories predict in addition the line AB which separates the spin-glass phase from the ferromagnetic phase. The ferromagnetic region corresponds exactly to the region of extended states of the electronic problem ($\langle\sigma_i\rangle \neq 0$ throughout the lattice). However for the spin-glass system the fully averaged moment $\langle\langle\sigma_i\rangle\rangle_J$ is zero. The quantity $\langle\langle\sigma_i\rangle^2\rangle_J \neq 0$ and defines the order parameter. ($\langle\langle\ \rangle\rangle_J$ denotes the configurational average.) It is this quantity now that is the long-range order parameter. It should be emphasized that the present analysis is not a substitute for a detailed theory of spin glass; it merely reproduces qualitatively some of the real features and thus it contributes somehow to a better understanding of this complicated physical system.

ACKNOWLEDGMENTS

We would like to thank M. H. Cohen and S. Kirkpatrick for pointing out to us the relation between the present result and the mean-field spin-glass problem. We also thank M. H. Cohen for numerous fruitful discussions during this investigation. Reference 8 was brought to our attention by A. Theodorou.

*Supported in part by NSF Grant No. DMR75-13343 and the Materials Research Laboratory of the NSF at The University of Chicago, by grants from the IBM and Xerox Corp. to The University of Chicago, and by NSF Grant No. GH-37264 at the University of Virginia, Charlottesville.

†Work started when one of us (E.N.E.) was visiting The University of Chicago.

[1]P. W. Anderson, Phys. Rev. 109, 1492 (1958).

[2]E. N. Economou and Morrel H. Cohen, Phys. Rev. B 4, 396 (1971).

[3]G. Theodorou and Morrel H. Cohen, Phys. Rev. B 13, 4597 (1976).

[4]D. C. Licciardello and E. N. Economou, Phys. Rev. B 11, 3697 (1975).

[5]R. Abou-Chacra, P. W. Anderson, and D. J. Thouless, J. Phys. C 6, 1734 (1973).

[6]E. N. Economou and Morrel H. Cohen, Phys. Rev. B 5, 2931 (1972).

[7]P. Lloyd, J. Phys. C 2, 1717 (1969).

[8]N. Pottier and D. Calecki, Solid State Commun. 9, 1489 (1971).

[9]E-Ni Foo, H. Amar, and M. Ausloos, Phys. Rev. B 4, 3350 (1971).

[10]J. A. Blackman, J. Phys. F 3, L31 (1973).

[11]J. A. Blackman, D. M. Esterling, and N. F. Berk, Phys. Rev. B 4, 2412 (1971).

[12]F. Brouers and J van der Rest, J. Phys. F 2, 1070 (1972).

[13]C. Papatriantafillou, E. N. Economou, and T. P. Eggarter, Phys. Rev. B 13, 910 (1976). The calculation is performed for one dimension, but it holds for any dimensions.

[14]A. R. Bishop and Abhijit Mookerjee, J. Phys. C 7, 2165 (1974).

[15]R. Haydock and Abhijit Mookerjee, J. Phys. C 7, 3001 (1974).

[16]A. R. Bishop, J. Phys. C 8, 3317 (1975).

[17]A. R. Bishop, Philos. Mag. 27, 1489 (1973).

[18]A. R. Bishop, Solid State Commun. 15, 1447 (1974).

[19]A. R. Bishop, Phys. Lett. A 49, 5 (1974).

[20]E. N. Economou, Phys. Rev. Lett. 28, 1206 (1972).

[21]J. T. Edwards and D. J. Thouless, J. Phys. C 5, 807 (1972).

[22]D. C. Licciardello and D. J. Thouless, J. Phys. C 8, 4157 (1975).

[23]N. F. Mott, *Metal-Insulator Transitions* (Taylor and Francis, London, 1974), and references therein.

[24]W. J. L. Buyers, T. M. Holden, E. C. Srensson, R. A. Couley, and R. W. H. Stevenson, Phys. Rev. Lett. 27, 1442 (1971).

[25]S. F. Edwards and P. W. Anderson, J. Phys. F 5, 965 (1975).

[26]D. Sherrington and S. Kirkpatrick, Phys. Rev. Lett. 35, 1792 (1975).

[27]J. M. Kosterlitz, D. J. Thouless, and R. Jones, Phys. Rev. Lett. 36, 1217 (1976).